

# Morphology and curvature of delta slopes in Swiss lakes: lessons for the interpretation of clinofolds in seismic data

ERWIN W. ADAMS\*, WOLFGANG SCHLAGER\* and FLAVIO S. ANSELMETTI†

\**Institute of Earth Sciences, Vrije Universiteit, De Boelelaan 1085, 1081 HV Amsterdam, The Netherlands (E-mail: adae@geo.vu.nl)*

†*Geologisches Institut, Swiss Federal Institute of Technology ETH, Sonneggstrasse 5, CH-8092 Zürich, Switzerland*

## ABSTRACT

Seismic surveys were conducted and bathymetric data obtained from four alpine lakes in Switzerland. The curvature of the delta slopes was analysed with mathematical equations. Linear or exponential profiles are observed, representing planar or concave morphologies respectively. Planar profiles are interpreted to represent sediment that rests at the angle-of-repose. The slope angle of these profiles shows a correlation with sediment calibre. Exponential profiles do not show a clear correlation between sediment calibre and slope angle; they do not rest at the angle-of-repose, and different kinds of sediment can rest at the same slope angle. At the transition from lower slope to toe-of-slope, the exponential equation fails to predict the present-day morphology. The toe-of-slope lies above the predicted trend. This is attributed to a drastic increase in turbidite deposition that provides additional sediment and raises the basin-floor profile above the predicted trend. The breaks between delta plain and slope are sharp, reflecting an abrupt change from transport by river flow and waves to gravity-driven transport. In these lakes, the base-level fluctuations relative to supply are small and insufficient to alter this sharp topographic break. The absence of sigmoidal profiles on the Swiss deltas is attributed to the high rate of progradation coupled with small fluctuations in base level.

**Keywords** Deltas, glacial lakes, lacustrine sedimentation, morphology, slopes, Switzerland.

## INTRODUCTION

The explanation of the origin of seismic reflection patterns is a recurrent problem in seismic interpretation. An important issue is the interpretation of the geometry of clinofolds in seismic sections in terms of style of deposition. Adams & Schlager (2000) proposed a hypothesis that a sigmoidally curved slope profile results from the interference between wave-dominated shelf transport and gravity-driven slope transport on the upper portion of the slope. This interference might be the result of base-level fluctuations. Strongly prograding systems or systems in which the shelf

break is fixed (Adams *et al.*, 1998) are not disturbed at the shelf break by this interference, and will therefore have a concave or planar slope morphology (Fig. 1). In the present report, this hypothesis is tested by studying the morphology and curvature of delta slopes in Swiss lakes.

Since Gilbert (1890) published his classical model of a prograding delta, numerous studies have focused on the depositional architecture of deltas (e.g. Postma, 1990), the processes acting in and on delta regimes (Nemec, 1990a; Prior & Bornhold, 1990) and the influence of sediment grain size on deltaic processes (e.g. Orton & Reading, 1993). Kenyon & Turcotte (1985) were

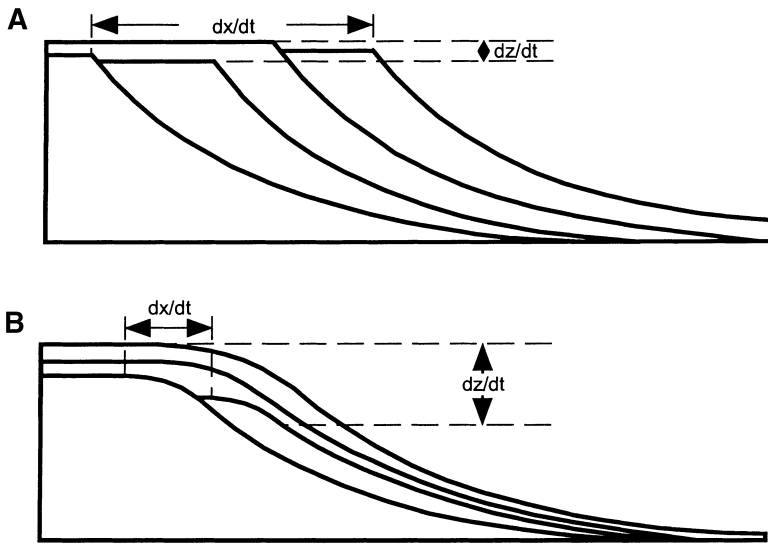


**Fig. 1.** Schematic cross-sections of prograding deltas. Sigmoidal profiles represent regular planar or concave-upward curvatures whose upper parts have been disturbed at the shelf break during base-level fluctuations. Wave-dominated transport on the shelf interferes with gravity-driven transport on the slope. (A) Rapidly prograding deltas exceed the fluctuations in base level and have concave-upward curvatures in cross-section. (B) Fluctuation in base level exceeds progradation rates, resulting in sigmoidal profiles.

among the first to model delta fronts numerically and to compare results with the geological record. Extensive modelling of the stratigraphic sequence geometry of clinoforms has been carried out (Ross *et al.*, 1995; Pirmez *et al.*, 1998; Driscoll & Karner, 1999). However, quantitative and empirical studies on slope morphology have received less attention.

Alpine lakes in Switzerland (Fig. 2) are ideal systems within which to analyse the subaqueous

slope morphology of lacustrine deltas and to study sedimentary processes acting in delta and basin environments; they can be viewed as analogues for small ocean basins (Hsü & Kelts, 1985) that are easy to monitor and study. Studying glacial lakes has the following advantages:

1. Alpine lakes, formed by glacial erosion, are filled with sediments at the end of a glacial period and during interglacial periods; sedimentation

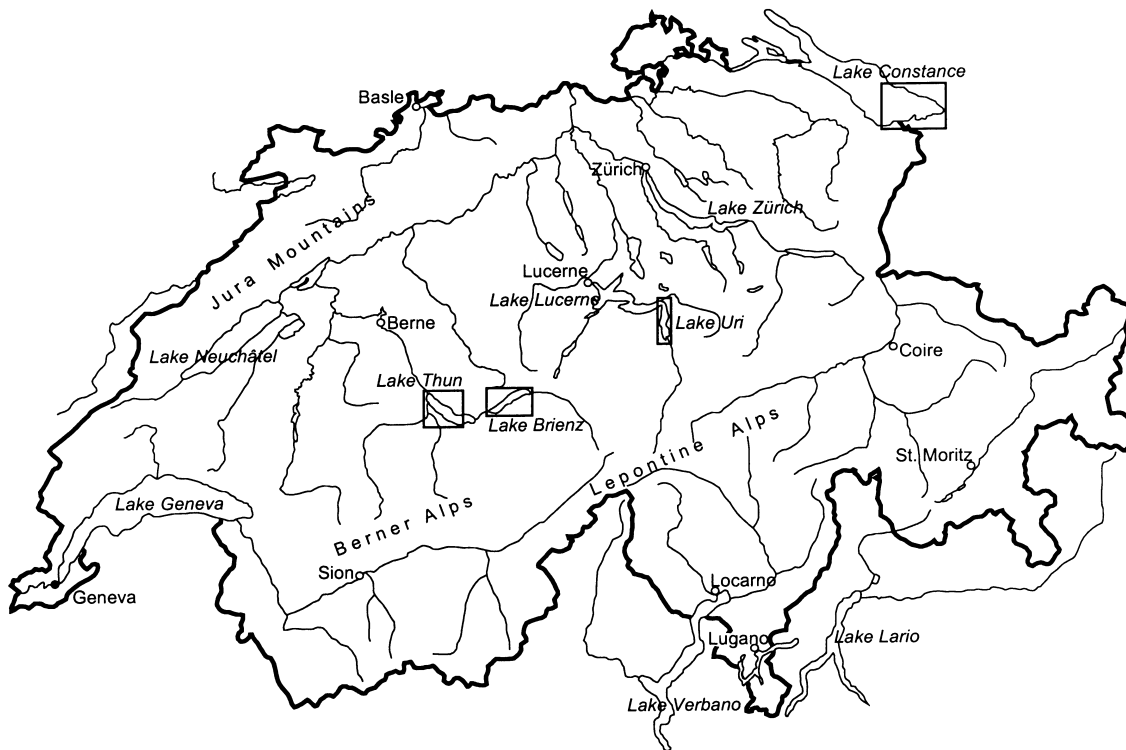


**Fig. 2.** Map of Switzerland showing the distribution of lakes and major rivers. The boxes indicate the lakes studied in this report.

rates are high in these alpine settings, producing rapidly prograding delta sequences.

2. There is a good record of lake-level fluctuation. Average daily, monthly and yearly values of the lake-level position have been recorded since 1870.

3. There is good control on the 'oceanographic' setting, such as major wind and current directions.

4. The recent history (including major slides and earthquakes) is well known in these areas.

In the present paper, the origin of delta slope morphology is examined, the processes acting in and on this depositional environment are reviewed, the influence of sediment calibre on slope morphology is examined and the significance of these lacustrine slopes as models of submarine slopes is discussed.

## SETTING

The genesis of alpine lake basins in Switzerland is variable (for a discussion, see Finckh *et al.*, 1984). In general, however, these basins owe their present condition to glacial erosion of valleys and subsequent sedimentation during the final stages of the last glacial periods and interglacial periods. Although sediments were deposited into these lakes before the Würm glacial period (Finckh & Kelts, 1976), only those of Holocene age are considered here. The morphology of these basins is more or less similar (see Table 1 for a summary of geomorphological parameters):

1. Alpine lakes have an elongate shape with steep lateral mountain slopes and axial deltas or outflows.

2. Distinct alluvial Gilbert-type deltas (Gilbert, 1890) are formed in front of the main tributaries. These input points provide most of the sediment influx.

3. Along the steep lateral mountain slopes, scree-apron deltas (Nemec, 1990b) are formed by lateral input points, which do not contribute much to the total amount of sediment delivered to the lake basins.

4. The main part of these lakes consists of a flat ponded basin floor.

5. The lakes are oligotrophic as a result of infusion of oxygen-rich surface waters entrained in turbidity currents (Sturm & Matter, 1972).

6. Thermal stratification occurs in summer, complete mixing in winter.

**Table 1.** Geomorphological parameters of four Swiss lakes.

	Length (km)	Width (km)	Depth (m)	Surface (km <sup>2</sup> )	Volume (km <sup>3</sup> )	Altitude (m)	Quaternary sediment thickness (m)	Major outflows	Major inflows	Delta	Average water flow (m <sup>3</sup> s <sup>-1</sup> )
Lake Uri*†	11	1–3	200	21	2.9	434	120–200	Branch of Lake Lucerne	Reuss Muota	Yes Yes	45 19
Lake Brienz‡	14	2–3	260	30	5.2	564	350–550	Aare	Aare	Yes Yes	33 19
Lake Thun§	18	2–3	215	48	6.6	558	200–300	Aare	Lütschine Aare	No	–
Lake Constance¶§	45	7–14	250	450	49.4	396	170	Rhine	Kander Rhine	Yes Yes	40 224

\* Data from Finckh *et al.* (1984).

† Data from Siegenthaler & Sturm (1991).

‡ Data from Matter *et al.* (1973).

§ Data from Matter *et al.* (1971).

¶ Data from Müller & Gees (1970).

§ Data from Müller (1966).

7. Strong thermal winds ( $6\text{--}11\text{ m s}^{-1}$ ) blow from the alpine range (Foehn winds). This is not the dominant wind direction but is one of the strongest wind systems in the Alps.

## METHODS

### Seismic profiling

High-resolution seismic profiling was conducted with a 3.5-kHz single-channel pinger containing four piezoelectric transducers. This pinger was loaded between two parallel inflatable hulls and pulled at a distance of 30 m from an inflatable Zodiac boat. Shot intervals were set at 0.5 s, triggered by a seismic processor (Octopus Marine 360). After A/D conversion, the signal was gained,

bandpass filtered (1400–6500 Hz) and printed with a graphic recorder (EPC 1086). The unfiltered analogue seismic signal was converted by the seismic processing unit into digital format at a sampling rate of  $42\ \mu\text{s}$  and stored on 8 mm Exabyte tapes in SEG-Y format. GPS co-ordinates were recorded and stored into the trace header. On a workstation, the digitally recorded data were processed using SPW processing software for Macintosh. Navigation was performed by map and GPS readings.

## RESULTS

The four lakes studied are Lake Uri (Urnersee), which is the south-eastern branch of Lake Lucerne (Vierwaldstättersee; Fig. 3A), Lake

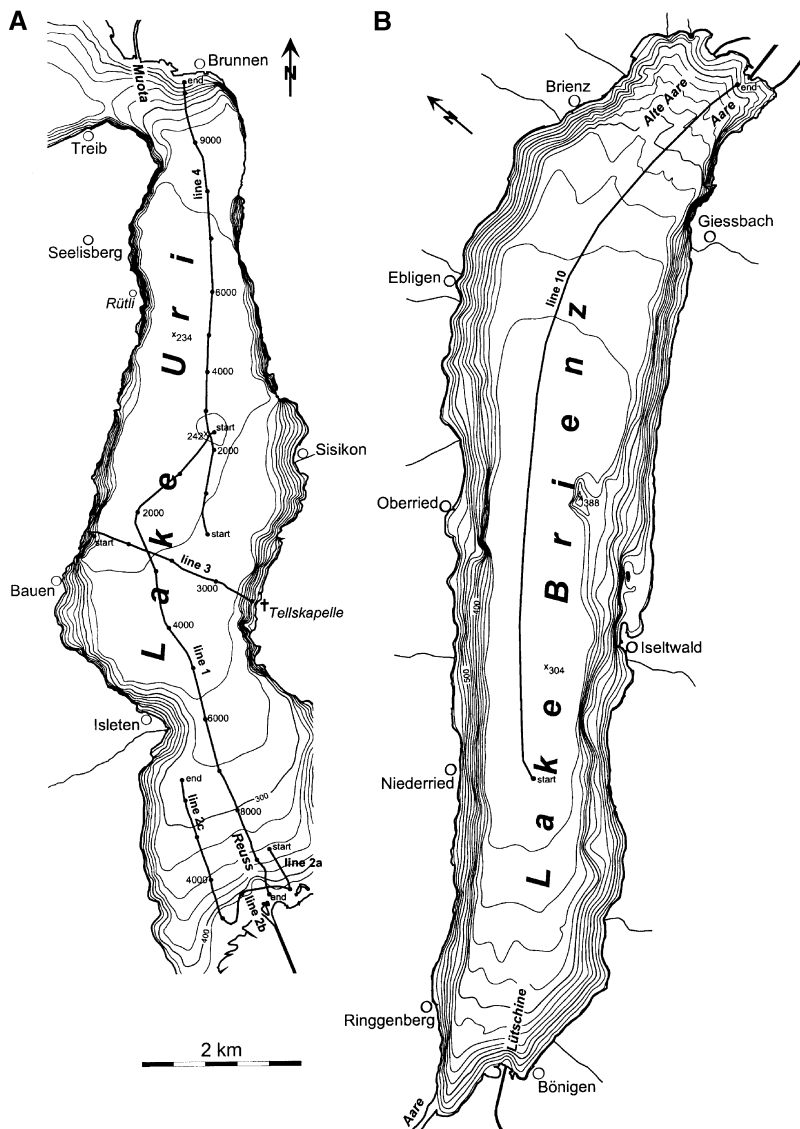


**Fig. 3.** Bathymetric maps. (A) Map of Lake Uri with the Reuss delta in the south and the Muota delta in the north. Note the tracklines of the seismic profiles. (B) Map of Lake Brienz with the Aare delta in the north-east and the Lutschine delta in the south-west. Note the trackline of the seismic profile. Contour lines are given in metres above sea-level.

Brienzi (Brienzersee; Fig. 3B), Lake Thun (Thunersee; Fig. 4A) and Lake Constance (Bodensee; Fig. 4B). Seismic surveys were conducted on Lake Uri and Lake Brienz; bathymetric data were obtained from Lake Thun and Lake Constance.

This presentation of results begins with the description of seismic and bathymetric data, followed by an analysis of slope curvature. Finally, information on sediment calibre and lake-level fluctuations is given.

### Lake Uri

Lake Uri (Fig. 3A) is 11 km long, 1–3 km wide and has a maximum depth of 200 m. Two main rivers, the Reuss in the south and the Muota in the north, provide most of the sediment influx and make distinct deltas in Lake Uri. Four 3·5 kHz single-channel seismic profiles were taken (the tracklines are shown in Fig. 3A).

Line 1 started in the basin in front of a smaller tributary, the Sisikon delta. Slump deposits derived from this lateral delta created relief on the basin floor (Fig. 5). Towards the Reuss delta,

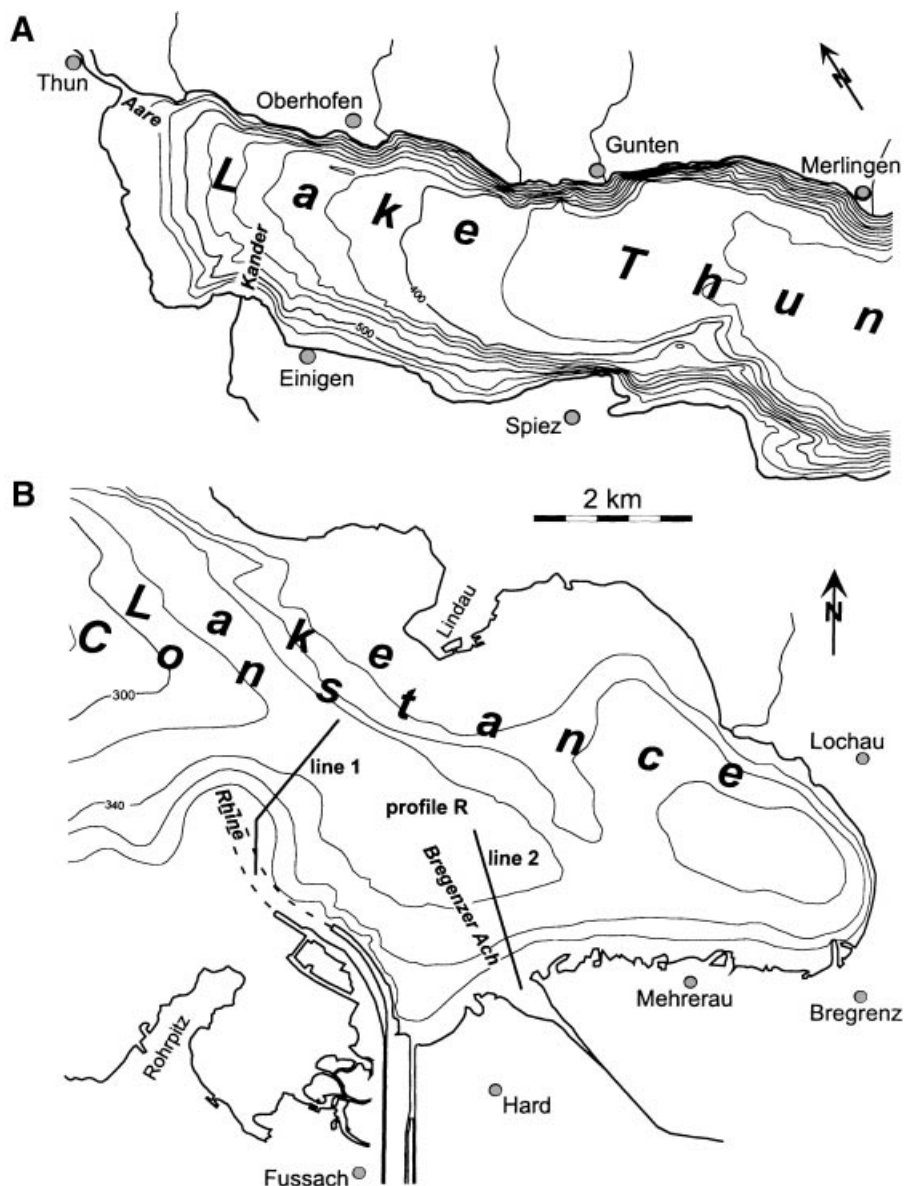


**Fig. 4.** Bathymetric maps. (A) Map of Lake Thun with the Kander delta in the north-west. (B) Map of Lake Constance with the Rhine and Bregenz Ach deltas in the south. Note the tracklines of the bathymetric profiles. Contour lines are given in metres above sea-level.

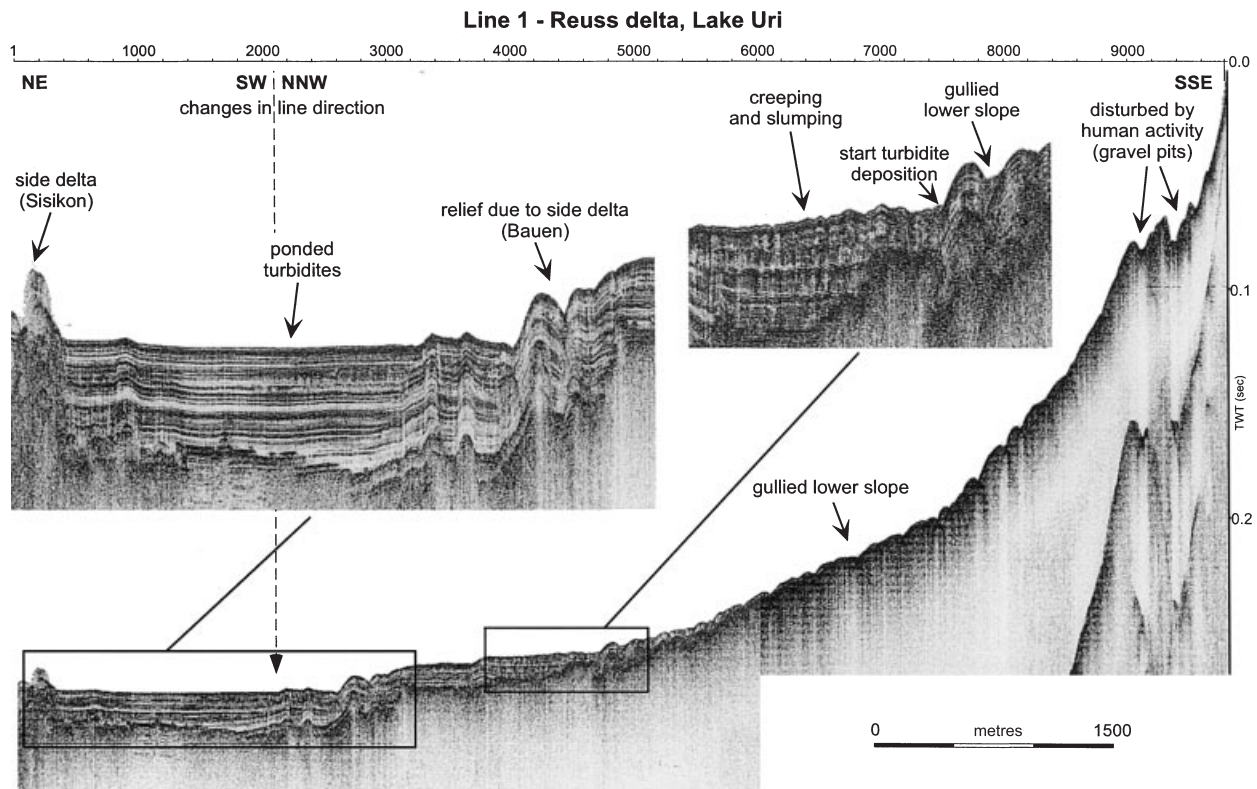


**Fig. 5.** Seismic line 1 across the basin floor and Reuss delta of Lake Uri. The topography on both sides of the basin floor results from sediment transport from lateral deltas, i.e. the Sisikon delta and the Bauen delta. The channel-like features are created by gravel mining. Note the change in line direction.

the Bauen delta (another lateral delta) has also influenced the topography of the basin. Reflections onlap against and drape over this topography. A layered seismic facies is observed only at the toe-of-slope and basin floor (Fig. 5). Layered sediments are fine and the surfaces sufficiently smooth to allow seismic energy to penetrate. At the toe-of-slope of the Reuss delta, deformed layering is evident (Fig. 5), interpreted to originate from slumping and creeping of turbidite deposits. On the lower slope, parabolic reflections are seen (Fig. 5), interpreted to be caused by ridges and gullies. On the upper slope, no such subsurface reflections are observed (Fig. 5) since coarse material reflects nearly all energy and creates many overlapping diffraction hyperbolae. Therefore, the absence of subsurface reflections on this steep upper slope might result from the presence of coarse material, such as coarse sand and gravel. Additionally, the large amount of organic matter brought in by the river might also cause a high content of free gas in the sediments, which does not favour penetration of the acoustic signal.

On the upper slope, which has a maximum slope angle of  $14^\circ$ , erosional pits are observed (Fig. 5). These pits are not submarine channels, but are formed by gravel mining. Line drawings of line 1 and line 2 (Fig. 6) show the morphology of the upper slope with gravel pits from 45 m to 72 m water depth, and delta channels up to 25 m deep. Line 3 (Fig. 7) crosses line 1 obliquely and, again, the influence of the Bauen delta can be seen on the relief of the basin.

A large slump is observed at the base of the Muota delta (Fig. 8) (cf. Siegenthaler & Sturm, 1991). The head of this slump deposit is 2 km from the delta front. Siegenthaler & Sturm (1991) interpreted this slump event to have occurred on the evening of 23 September 1687. The impact of the slump triggered a surge with a height of 5 m. The Muota delta has been inactive since this event, and the resulting sharp nick of the slump scar is still evident. A drape of mud on the middle slope and slumps on the lower slope are the only evidence of sedimentation after this event (Fig. 8). A drape of fine sediment (distal turbidites?) is observed on the inactive toe-of-slope. Creep has deformed the basal part of this drape.

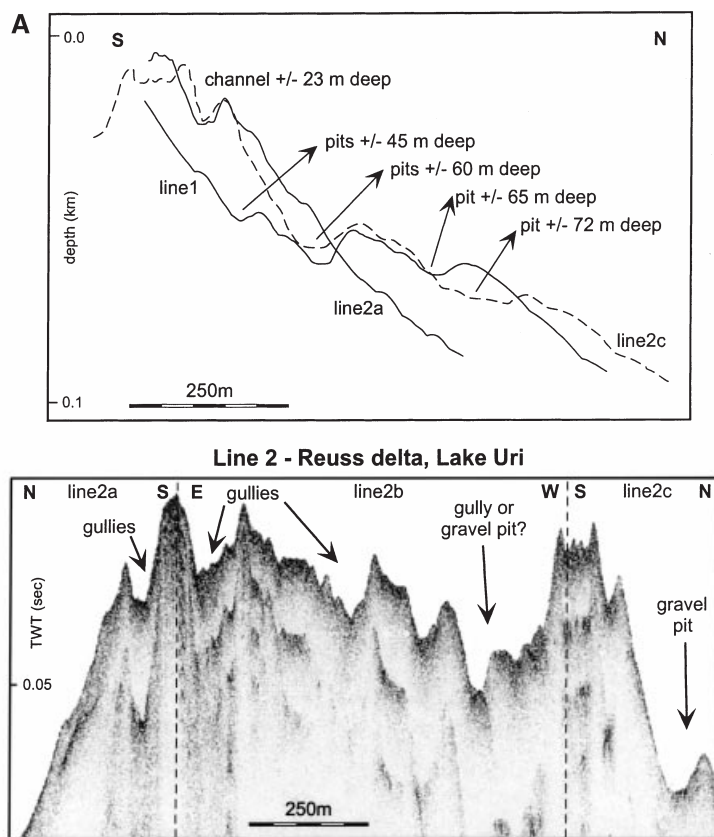


**Fig. 6.** Seismic line 2 across the Reuss delta of Lake Uri. (A) Line drawings of lines 1 and 2 show the gravel pits and submarine channel of the Reuss delta. (B) Seismic line 2 shot across the slope and delta front of the Reuss delta. Note the steep upper slope, gullies and gravel pits.

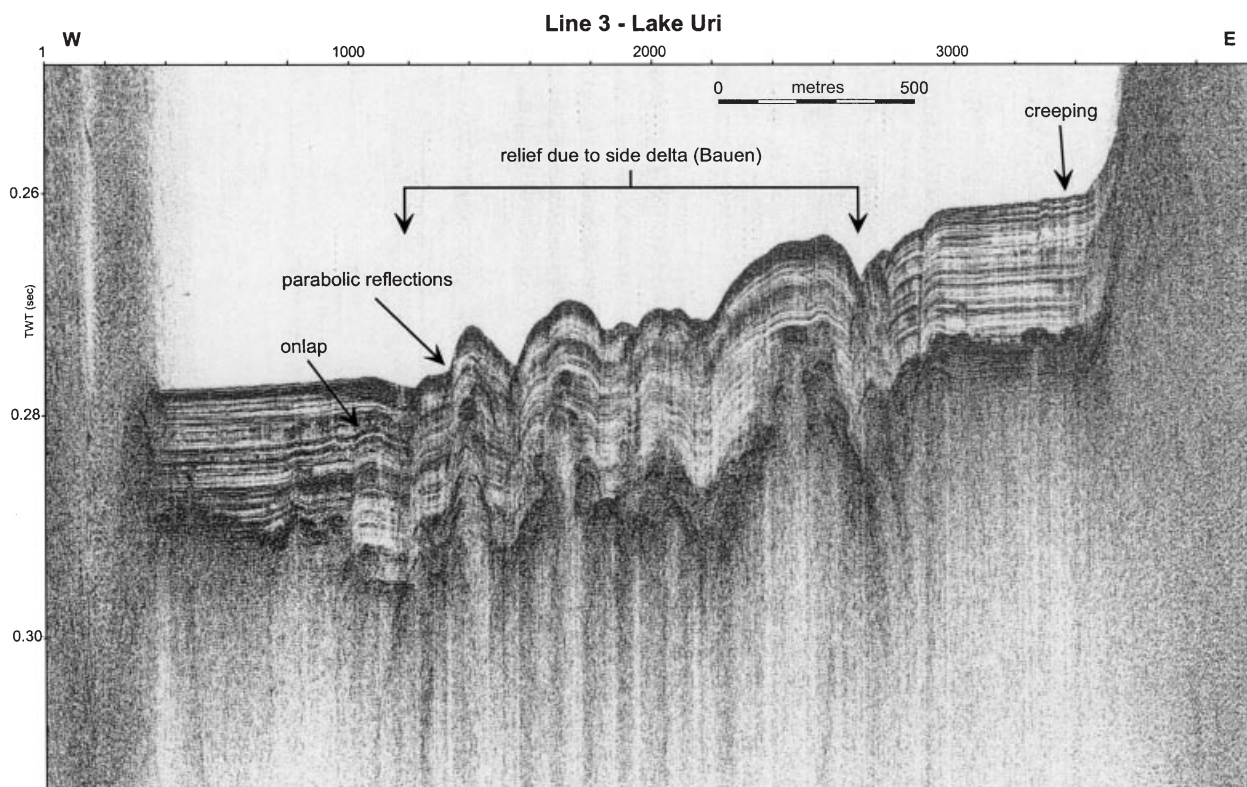


**Fig. 7.** Seismic line 3 across the basin of Lake Uri. The relief in the centre of the basin is created by sediment transport from the Bauen delta. Note the steep lateral slopes created by glacial erosion.

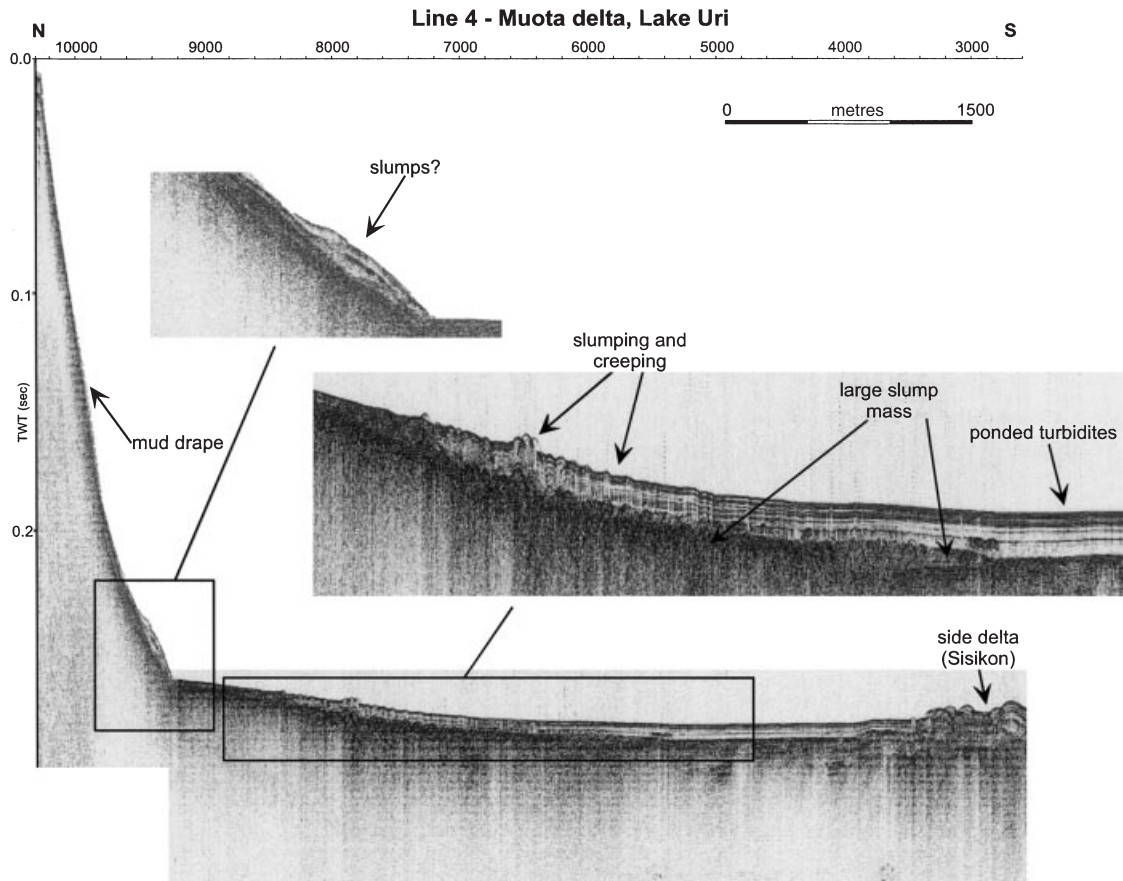


**Fig. 8.** Seismic line 4 across the basin floor and Muota delta of Lake Uri. The slump deposits, deposited by the Sisikon delta, can be seen in the south of the profile. Note the large buried slump mass and the sharp nick point of the slump scar at the toe-of-slope.

### Lake Brienz

Lake Brienz (Fig. 3B) is 14 km long, 2–3 km wide and has two main inflows: the Aare and the Lütschine. These two rivers provide Lake Brienz with most of its sediment influx and make distinct deltas in the north-east and the south-west respectively. Around 1900 AD, the inflow of the Aare was moved  $\approx 500$  m southwards (Fig. 3B). Scree-apron deltas (Nemec, 1990b) are observed along the steep lateral slopes, and the main part of the lake consists of a flat ponded basin floor with a depth of 260 m.

A seismic profile is shown in Fig. 9 (cf. Schmidt, 1998). The upper slope of the Aare delta has a maximum slope angle of  $17^\circ$ . A depositional centre, represented by a zone of low-amplitude reflections, is observed below the upper slope. The lower slope is cut by gullies and, at the toe-of-slope, deformation by creeping and slumping of turbidite deposits can be seen. In the south-western part of this profile, turbidite

deposits of the Aare and Lütschine delta apparently interfinger (Fig. 9; Sturm & Matter, 1978; Schmidt, 1998). The south-western end of the profile shows the toe-of-slope of the Lütschine delta, deformed by creeping and slumping. The morphology of the Lütschine delta was obtained from bathymetric data (Sturm, 1976).

### Lake Thun

Lake Thun (Fig. 4A) is 18 km long, 2–3 km wide and has a maximum depth of 215 m. Two major rivers, the Aare in the south-east and the Kander in the north-west, supply the majority of the water to this basin. However, as the Aare is connected to Lake Brienz where it deposits most of its sediment, the sediment influx to Lake Thun is mostly provided by the Kander. A delta is formed in front of this river. Its bathymetry was obtained from the literature (Sturm & Matter, 1972). The Kander has flowed into Lake Thun only since 1714. Since then, a

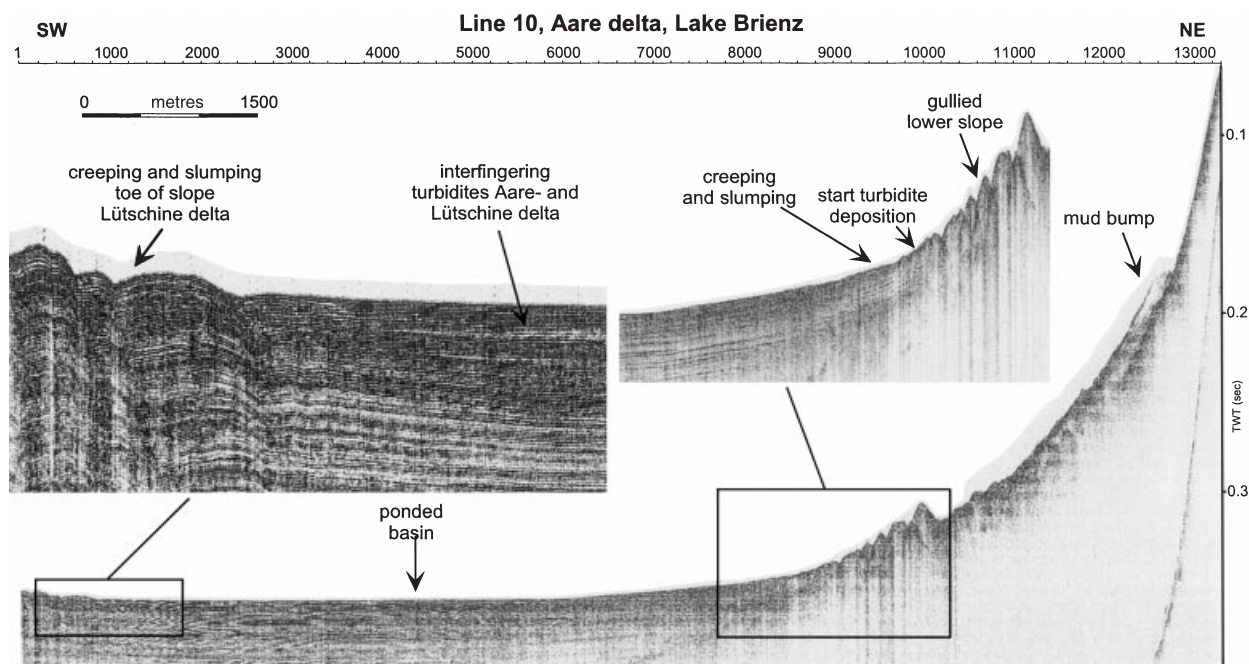


**Fig. 9.** Seismic line 10 across the basin and Aare delta of Lake Brienz. A depositional centre is observed below the steep upper slope at 0.2 s. This depositional centre is interpreted as being a mud bulge, because it is represented by a zone of low-amplitude reflections. The lower slope is dissected by gullies and, at the toe-of-slope, deformation of turbidite deposits can be seen. In the south-western part of this profile, turbidite deposits of the Aare and Lüttschine deltas interfinger. The strange seismic pattern in the SW part of the large profile is artificial.

concomitant increase in turbidity current activity has changed the environment of the deep lake from eutrophic to oligotrophic as a result of the infusion of oxygen-rich surface waters entrained in turbidity currents (Sturm & Matter, 1972). The main part of the lake consists of a flat ponded basin floor.

### Lake Constance

Lake Constance (Fig. 4B) is located on the boundary between Germany, Austria and Switzerland and is an order of magnitude larger than the other three lakes described above. One of Europe's largest rivers, the Rhine, flows into this 45-km-long, 7- to 14-km-wide and 250-m-deep lake. The entry point of the Rhine was artificially altered in 1900 AD, and a distinct Gilbert-type delta has formed in front of this new inlet. Bathymetric data were obtained from this part of the lake (Meixner, 1991). Two profiles were constructed from these charts: a profile across the Rhine delta and one across the Bregenz Ach delta.

### Curve-fitting the delta slopes

The curvature of the delta slopes was analysed by fitting equations to them. In a survey of the recent

morphology of submarine slope profiles, it was found that three simple mathematical equations can describe planar, concave and sigmoidal first-order morphologies (cf. Adams & Schlager, 2000). A concave profile is best described by an exponential function, whereas a Gaussian distribution was found to fit a sigmoidal morphology well. The most simple slope geometry is a planar surface, which in cross-section is described by the equation of a straight line. The lower slope of such planar profiles passes into the horizontal by a segment of concave curvature, which is again well described by an exponential function. The boundary between the planar upper slope and the exponential lower slope is determined at the point of deviation from the linear trend.

In order to curve-fit the delta slopes, the lake-floor profile of the seismic profiles was digitized and two-way travel time converted into depth by using  $1.50 \text{ km s}^{-1}$  as the sonic velocity of water. All three equations described above are curve-fitted to each digitized delta slope. A  $\chi^2$ -test and correlation coefficients from non-linear least-squares regression were used to determine which equation best fitted the profile. The slope is defined as the area between the break and the toe-of-slope, which are defined in strict analogy to shelf break and continental rise respectively. The

break is defined as the point of marked increase in gradient relative to the delta plain (Vaney & Stanley, 1983). The upper limit of the toe-of-slope is defined as the point where the angle of the slope drops below the tangent of 0.025 (Heezen et al., 1959).

The four lakes studied contain seven deltas (see Table 1). The slope profiles of these seven deltas and their curve-fits are plotted in Fig. 10. Five profiles are best fitted with a combination of the equation of a straight line fitted to the upper slope and an exponential function fitted to the lower slope (Fig. 10A–E). The maximum slope inclination of the planar upper slopes varies from 14° to 26°. The lower slopes, which are gullied, follow the exponential trend. However, the surface of these profiles is somewhat irregular. The two profiles of Lake Constance show a good fit with

the exponential function fitted to the whole profile (Figs 10D and 10F). The maximum slope inclination, measured at the upper slope of these profiles, is 6°.

The origin and quality of the data differ for the seven delta slopes studied. Three profiles were taken from seismic profiles. Four profiles were taken from bathymetric charts with different resolutions: two with 10 m and two with 1 m contour spacing. Despite these different resolutions, however, all observed breaks between the topset delta plain and the delta slope are sharp (Fig. 11).

### Sediment calibre

A triangular diagram shows the sediment calibre of the deltas (Fig. 12). Lakes Uri, Thun and Brienz

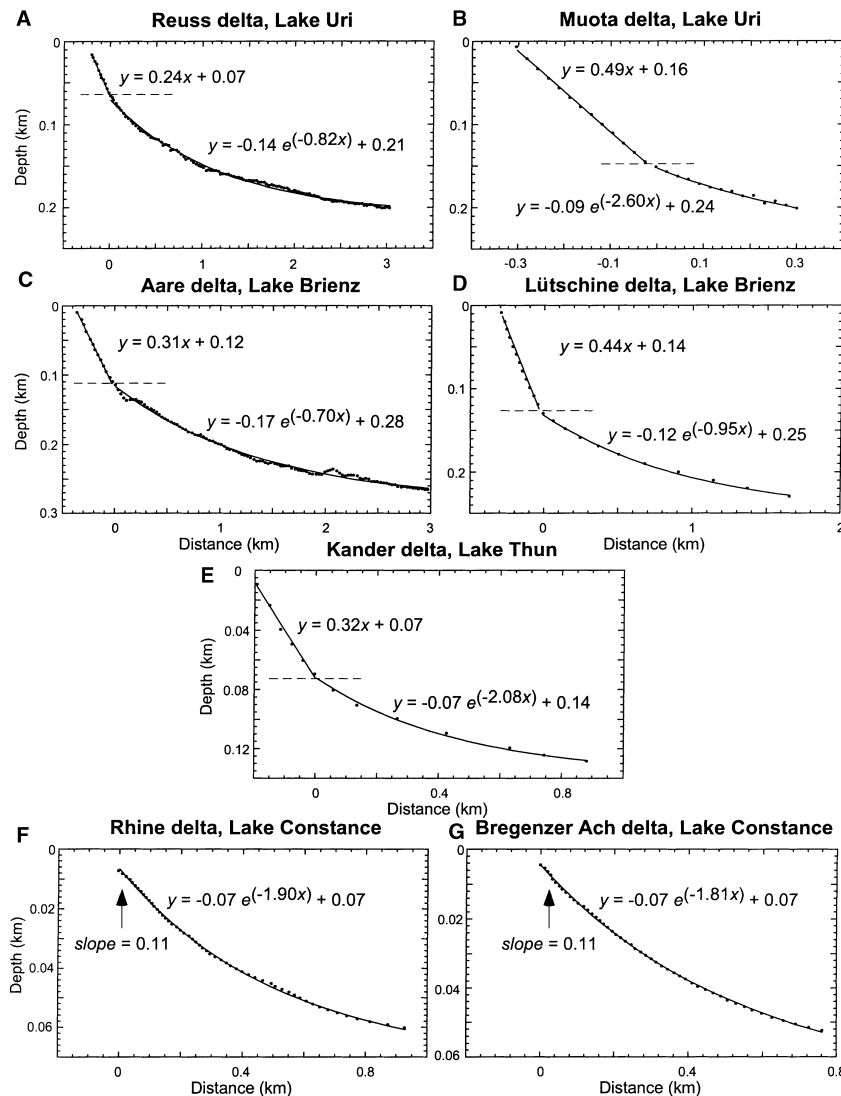


**Fig. 10.** Curve-fits of slope profiles. Dots are measured slope data; lines are curve-fits. (A–E) Combination of the equation of a straight line fitted to the upper slope and an exponential function fitted to the lower slope. (F and G) Exponential curve fitted to the whole profile. (D) Data from Sturm (1976). (E) Data from Sturm & Matter (1972). (F and G) Data from Meixner (1991).

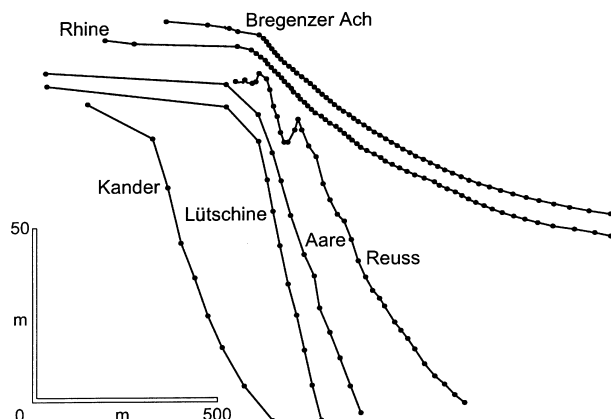


**Fig. 11.** Details of the upper slopes of the deltas shown in Fig. 10. All have sharp breaks between delta plain and slope. The origin and quality of the data vary. The Reuss and Aare deltas were taken from seismic profiles. The Lüttschine and Kander deltas were taken from bathymetric profiles with 10-m contour spacing. The Rhine and Bregenzer Ach deltas were taken from a bathymetric chart with 1-m contour spacing. Lüttschine delta, data from Sturm (1976); Kander delta, data from Sturm & Matter (1972); Rhine and Bregenzer Ach deltas, data from Meixner (1991).

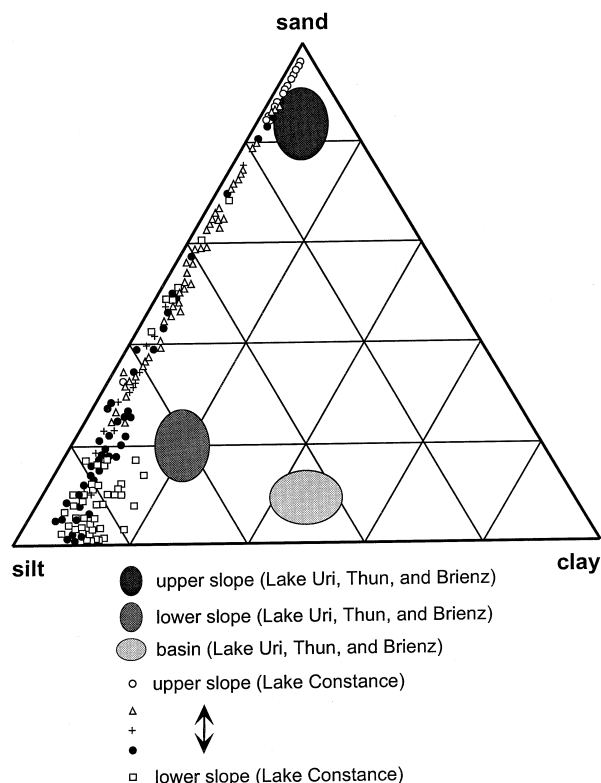


**Fig. 12.** Triangular composition plot. The upper slopes of the deltas are all sand dominated, and the lower slopes are silt dominated. Data from Förstner *et al.* (1968), Siegenthaler & Sturm (1991) and Sturm & Matter (1972, 1978).

have more or less the same sediment calibre (Sturm & Matter, 1972, 1978; Siegenthaler & Sturm, 1991). The delta plains of these three lakes consist of sand and gravel. The upper slopes are sand dominated, the lower slopes silt dominated. The basins consist of varved sediments of alternating laminated mud and silt layers, with intercalations of sandy turbidites. Sediments in Lake Constance are finer grained and better sorted (Müller, 1966; Förstner *et al.*, 1968). The slopes consist mostly of fine sand. Gravel and mud are absent.

### Lake-level fluctuation

The fluctuation in base-level in alpine lakes is determined by two factors: the fluctuation in lake level, which is mostly determined by the variation in total water discharge, and the effective wave base of wind-generated waves.

The measured lake-level fluctuations of the last century are shown in Fig. 13. In Lake Brienz and Lake Constance, the lake-level fluctuation between summer and winter is 1 m and, over years and decades, is 2 m. In Lake Uri and Lake Thun, the lake level fluctuates 0.4 m between summer and winter and 1 m over years and decades. With wind speeds of the order of  $6\text{--}11\text{ m s}^{-1}$  and a fetch of 10–40 km, the effective wave base ( $\approx 50\%$  of the wave length) is of the order of 1.5–4 m (Sly, 1978; Bearman, 1989). Therefore, the total base-level fluctuation in these lakes reaches to a depth of about 2.5–6 m.

### DISCUSSION

The goal of studying alpine lakes is to use these natural laboratories for studying the depositional anatomy of lake deltas and to compare these findings with submarine slopes. In this section, the sedimentary processes acting in alpine lakes are examined, followed by the influence of sediment calibre on delta-slope morphology. Finally, the relevance of these lacustrine delta slopes for the interpretation of submarine slopes is discussed.

### Sedimentary processes

Six depositional zones can be recognized in these lacustrine basins: an alluvial topset plain; a planar upper slope; an exponential lower slope; a toe-of-slope; a basin floor; and a lateral slope. The processes acting in these depositional zones are reviewed below.

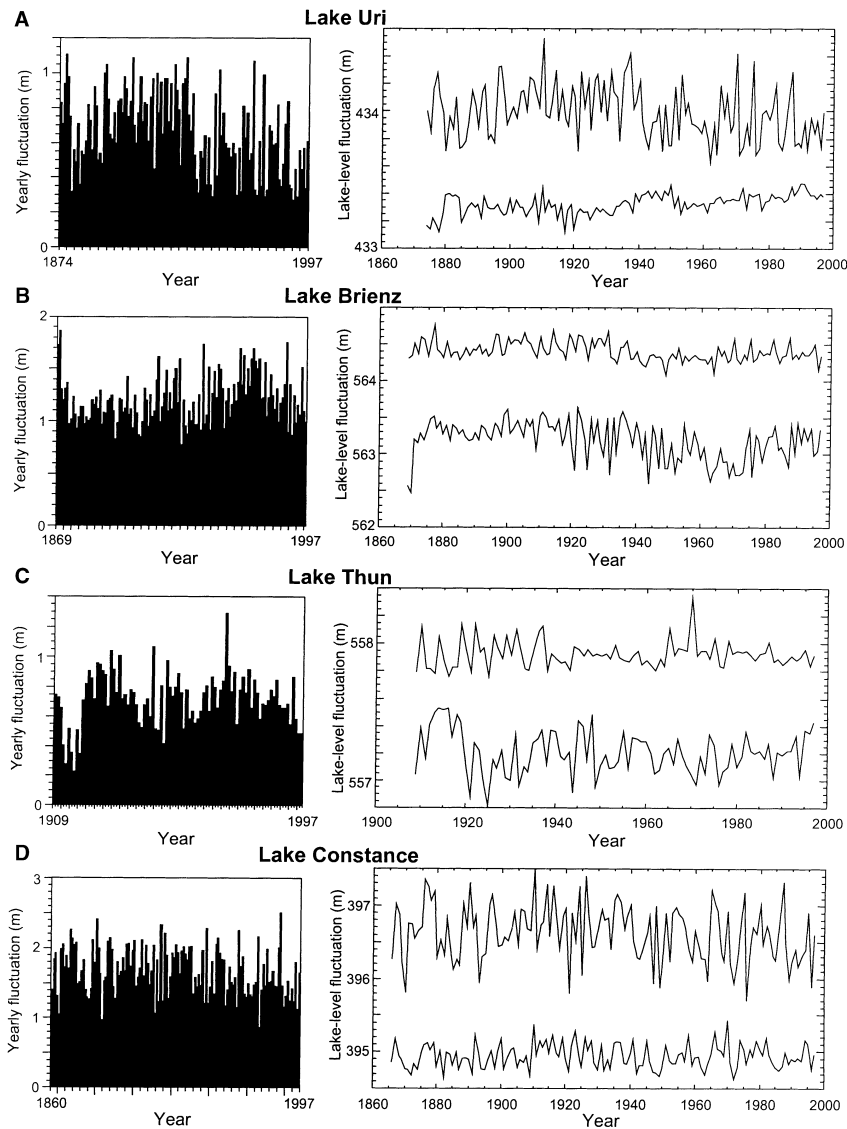


**Fig. 13.** Fluctuations in lake level in the last century for the four Swiss lakes. (A) Lake Uri. (B) Lake Brienz. (C) Lake Thun. (D) Lake Constance. Data obtained from the Swiss National Hydrological and Geological Survey. Upper line – summer month of highest water level (normally June); lower line – winter month of lowest water level (normally February).

### Alluvial plain

On the alluvial plain, coarse sediments are deposited, whereas the finer fractions are transported to the delta front by rivers. At the delta front, the cold dense water of the inflow loses its power, and the sand fraction is deposited on the upper slope. The finer sediments stay in suspension and are transported in density currents further into the lake and settle on the basin plain. Owing to the summer density stratification, some of these density currents travel into the lake as interflows (Sturm & Matter, 1978); others travel downslope as turbidity currents. More powerful and higher discharges, resulting from heavy rainfalls or spring meltwater, can bring gravel and coarse sand to the delta front where it is deposited on the upper slope.

### Planar upper slope

The upper slope consists predominantly of sand, with minor amounts of gravel, silt and clay. The planar shape of the upper slope is interpreted as being at the angle-of-repose. Non-cohesive planar slopes at the angle-of-repose behave as one system in a self-organized critical state (Bak *et al.*, 1988); a minor addition of sediment may lead to adjustments of grain packing anywhere on the slope. The slope inclination is fixed for these systems, and the sediment transport rate adjusts to maintain these maximum slope inclinations, i.e. the transport rate by avalanches, the dominant slope process, increases with an increase in sediment delivery to this critical pile (Allen, 1970).

*Exponential lower slope*

Sediment, transported by avalanches on the upper slope, comes to rest on the non-critical lower slope. Turbidity currents generated on the upper slope, or triggered by avalanches, which arrive from the upper slope, shape the lower slope. The exponential curvature of this part of the slope is attributed to the exponential decay of transport capacity or competence of the significant transport mechanisms (mainly turbidity currents). Whether the capacity or the competence of these transport processes is the main control remains open (cf. Hiscott, 1994). The zone

of low-amplitude reflections below the planar upper slope of the Aare delta in Lake Brienz (Fig. 9) is interpreted as being a depositional centre where fine muddy sediments from suspension plumes and interflows accumulate. If this pile reaches its critical angle, slope failure occurs, and turbidity currents are triggered, which in turn flow through the gullies and deposit their load on the basin floor.

*Toe-of-slope*

At the transition from gullied lower slope to toe-of-slope are the first continuous subsurface

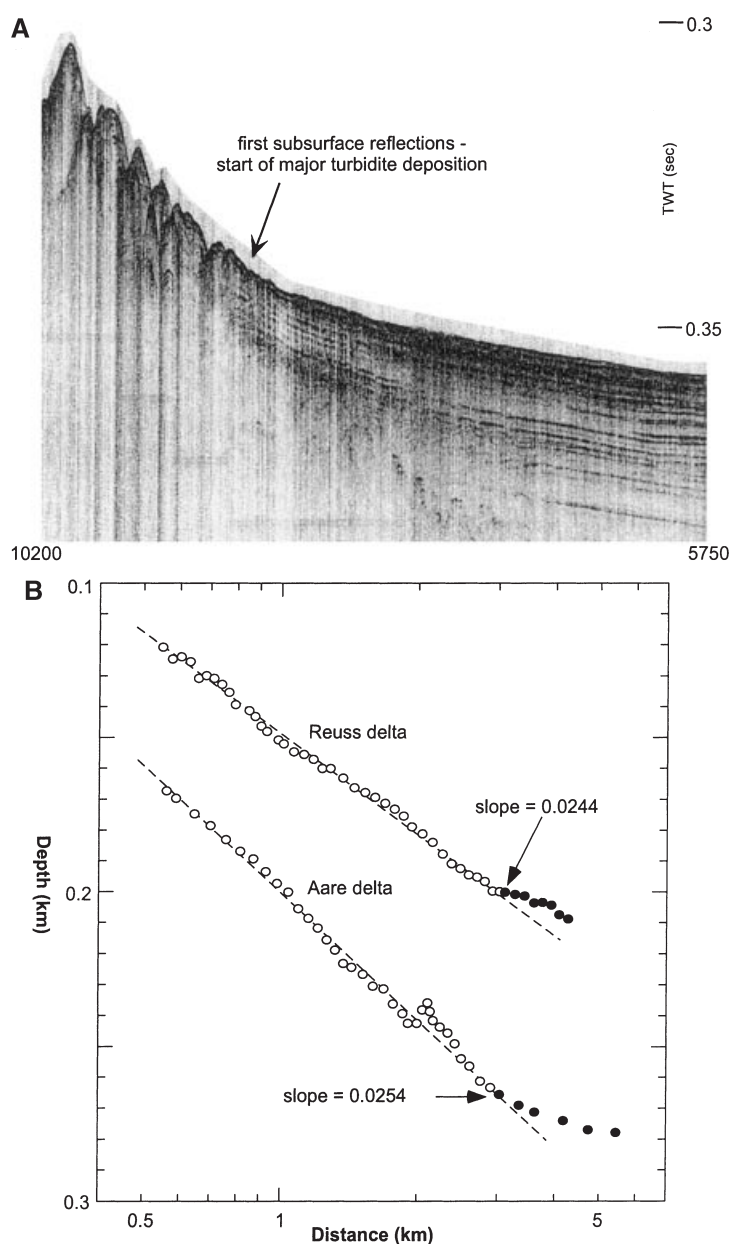


**Fig. 14.** Start of major turbidite deposition at the transition from lower slope to toe-of-slope. (A) Aare delta in Lake Brienz; lateral scale is 4000 m. The first appearance of subsurface reflections is observed at the transition from gullied lower slope to toe-of-slope. A layered seismic facies onlaps the gullied lower slope. (B) Log-log plot of digitized data from three delta slopes fitted with an exponential function. At the toe-of-slope, a systematic deviation can be seen, in that the distal part of the slope lies above the predicted exponential trend. These points are at the same location as the appearance of the first subsurface reflections, which have an angle of  $1.4\text{--}1.6^\circ$ . This deviation is attributed to a drastic increase in turbidite deposition at this slope angle, which raises the basin floor above the predicted trend.

reflections. This layered seismic facies onlaps the gullied lower slope (Fig. 14A). The first appearance of subsurface reflections is interpreted as a drastic increase in turbidite deposition, not as a lateral change into an opaque facies resulting from a lateral change in grain-size (Schlager & Chermak, 1979). Figure 14B shows a semi-log plot of digitized data from the lower slope and toe-of-slope of the Reuss and Aare deltas. An exponential trend plotted on semi-log paper plots as a straight line. At the toe-of-slope, these profiles exhibit a systematic deviation, in that the distal part of the slope lies above the predicted exponential trend. The points of deviation from the exponential trend coincide with the appearance of the parallel reflections and have an angle of 1.4–1.6°. The deviation from the exponential trend is attributed to the start of major turbidite deposition, raising the basin floor above the predicted trend (Schlager & Camber, 1986). From the limited information available on sediment texture, it cannot be inferred whether the coarse fraction is already deposited on the slope and only the finer fraction bypasses the slope, but a drastic increase in turbidite deposition probably starts at the point of deviation. The slope angle at this point agrees with the definition of the boundary between continental slope and continental rise of Heezen *et al.* (1959). Creeping and slumping can deform these turbidite deposits, which indicates that deposition from turbidity currents alone does not necessarily lead to a stable slope profile.

### Basin floor

At the basin floor, fine perennial sediments and turbidites are deposited. Slump deposits derived from the lateral slopes create topographic highs on the basin floor that are onlapped by turbidites and draped by perennial sediments.

### Lateral slope

Most of the sediment influx is provided by the axial deltas (i.e. a delta prograding in the direction of the long axis of the lake). However, where lateral rivers deposit sediment, scree-apron deltas are formed, which can be viewed as the underwater extension of mountain-slope scree slopes (Nemec, 1990b). The influence of this lateral deposition increases in a basinward direction, i.e. the small tributaries do not influence the progradation of the major deltas. Slump deposits derived from these lateral slopes create topographic highs on the basin floor.

## Slope curvature and sediment calibre

It is evident that an exponential function or a combination of a straight-line segment with an exponential segment describes the slope profiles of the lacustrine deltas well. It is noted furthermore that the planar segments of the slope profiles are best interpreted as sediments that rest at the angle-of-repose. The most important factor influencing the angle-of-repose of sediments is the sediment texture, i.e. grain-size, sorting, shape (Chandler, 1973; Kirkby, 1987; Kenter, 1990). Kirkby (1987) estimates the angle-of-repose for sand- and silt-dominated sediments to be 25°, and that of clay-dominated sediments to be 10° (Fig. 15). The five linear silt- and sand-dominated slope profiles in this study have maximum slope angles ranging from 14° to 26°, in the range predicted for silt- and sand-rich systems.

The Rhine delta of Lake Constance consists of terrigenous sand and silt (Fig. 12). The entry point of the Rhine was changed artificially in 1900 AD. Since then, the delta slope has prograded 1800 m into water 60 m deep (Müller, 1966). The maximum slope angle of the exponential profiles is 6°. The upper slope cannot be described by a linear equation, and the measured slope angle does not agree with the angle-of-repose for silt- and sand-dominated slopes. Müller (1966) reported that the Rhine delta has become steeper with time. It is surmised that the system has not yet reached its maximum inclination; the sediment calibre is more or less the same as the other delta slopes (Fig. 12), but the curvature is different (Fig. 10).

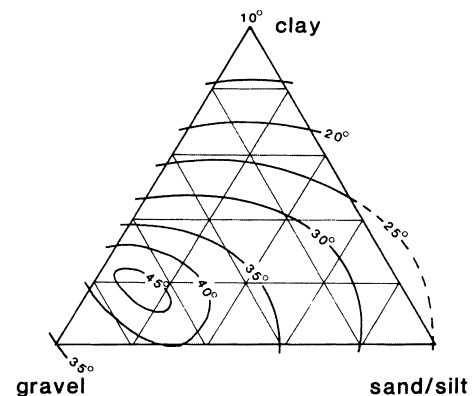


Fig. 15. Generalized relationship between grain-size and angle of internal friction. The angle-of-repose for sand- and silt-dominated sediments is 25° and that of clay-dominated sediments is 10° (modified according to Kirkby, 1987; taken from Kenter, 1990).

Table 2. Sedimentological parameters of lacustrine and submarine slopes.

Location	Line name	Data source	Setting	WLF (m)	Profile	Break depth (m)	Slope height (m)	Slope angle (°)	Sediment calibre upper slope	Reference
Reuss delta, Lake Uri, Switzerland	Line Uri-1	Seismics	Lake	1.1*	L-C	16	184	14	(cl), si, f-m.sd (c.sd, gr)	This study; Siegenthaler & Sturm (1991)
Muota delta, Lake Uri, Switzerland	Line Uri-4	Seismics	Lake	1.1*	L-C	8	194	26	(cl), si, f-m.sd (c.sd, gr)	This study; Siegenthaler & Sturm (1991)
Aare delta, Lake Brienz, Switzerland	Line Brienz-10	Seismics	Lake	1.9*	L-C	9	257	17	(cl), si, m-c.sd, gr	This study; Sturm & Matter (1978)
Lütschine delta, Lake Brienz, Switzerland	Lütschine profile	Bathymetric map	Lake	1.9*	L-C	10	221	24	(cl), si, m-c.sd, gr	Sturm (1976); Sturm & Matter (1978)
Kander delta, Lake Thun, Switzerland	Kander profile	Bathymetric map	Lake	1.3*	L-C	10	119	18	(cl), sd (gr)	Sturm & Matter (1972)
Rhine delta, Lake Constance, Austria	Line 1	Bathymetric map	Lake	2.5*	C	7	53	6	c.si, f-m.sd	Meixner (1991); Förstner <i>et al.</i> (1968)
Bregenzer Ach delta, Lake Constance, Austria	Line 2	Bathymetric map	Lake	2.5*	C	4	46	6	c.si, f-m.sd	Meixner (1991); Förstner <i>et al.</i> (1968)
Losna delta, Lake Losna, Norway	Losna profile	Echo sounder	Lake	-	L-C	2	27	37	c.si-m.sd	Bogen (1983)
Atnsjø delta, Lake Atnsjø, Norway	Atnsjø profile	Echo sounder	Lake	-	L-C	1	27	32	c.si-m.sd	Bogen (1983)
Alta delta, Finnmark, Norway	Alta profile	Echo sounder	Fjord	2.5†	L-C	3-5	100	35	vf-f.sd	Comer <i>et al.</i> (1990)
Bella Coola delta, North Barentinck Arm, Canada	Bella Coola profile	Echo sounder	Fjord	5.9†	C	15	240	15	cl, si, sd, gr	Kostaschuk & McMann (1983)
South-east South Island, New Zealand	Line A14E	Seismics	Marine	-	C	235	325	9	si, sd	Carter (1988)
Weddell Sea, Antarctica	Line 90060	Seismics	Marine	-	C	450	1740	3	cl, si, sd, gr	De Baptist <i>et al.</i> (1997); Bart <i>et al.</i> (1999)
Scotian Slope, Canada	Line C-C'	Seismics	Marine	-	L-C	185	1310	7	cl, si (sd)	Jansa (1991); Mosher <i>et al.</i> (1994)
Ganges-Brahmaputra delta, Bengal shelf	Line A	Seismics	Shelf	-	S	41	54	0.19	cl, si, vf-f.sd	Kuehl <i>et al.</i> (1997); Michels <i>et al.</i> (1998)

WLF, water-level fluctuation; L, linear profile; C, concave; S, sigmoidal; gr, gravel; sd, sand; si, silt; cl, clay; vf, very fine; f, fine; m, medium; c, coarse; O, present but not abundant.

\*Lake-level fluctuation.

†Spring-tide range.

Table 2 summarizes the sedimentological parameters of the seven deltas of the Swiss lakes together with eight other lacustrine and submarine slopes. Figure 16 shows the sediment calibre and maximum slope inclination of these profiles. The trend that non-cohesive linear profiles have higher slope angles than cohesive profiles can be seen (Fig. 16A). A profile from the Scotian Slope

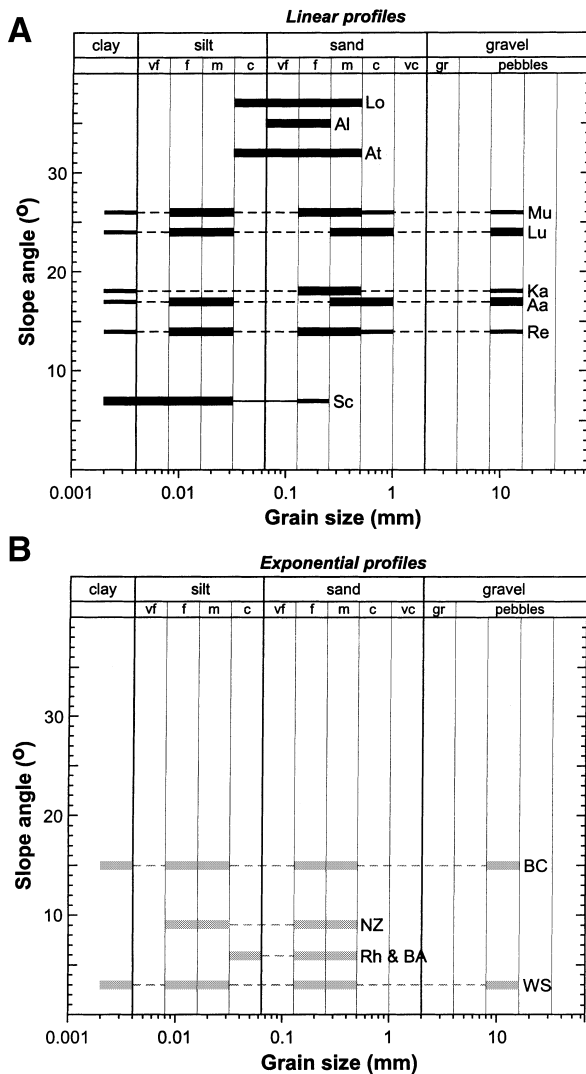


**Fig. 16.** Sediment calibre vs. slope angle. (A) The linear profiles show the trend that cohesive sediments have a lower angle-of-repose than non-cohesive sediments. (B) The exponential profiles do not show a clear correlation between sediment calibre and slope angle. Aa, Aare delta; Al, Alta delta; At, Atnsjø delta; BA, Bregenzer Ach delta; BC, Bella Coola delta; Ka, Kander delta; Lo, Losna delta; Lu, Lütschine delta; Mu, Muota delta; NZ, New Zealand, south-east South Island; Re, Reuss delta; Rh, Rhine delta; Sc, Scotian Slope; WS, Weddell Sea. See Table 2 for the sedimentological parameters of these slopes.

(Jansa, 1991), which is clay and silt dominated (Mosher *et al.*, 1994), has an angle of  $7^\circ$ . The lacustrine deltas from Switzerland with mixtures of silt and sand have slope angles ranging from  $14^\circ$  to  $26^\circ$ . The sand-dominated profiles, without clay or silt, from lakes or fjords in Norway (Bogen, 1983; Corner *et al.*, 1990) have maximum slope angles of  $35^\circ$  at the upper slope. The exponential profiles from Lake Constance, a fjord delta in Canada (Kostaschuk & McMann, 1983), New Zealand (Carter, 1988) and the Weddell Sea (De Batist *et al.*, 1997; Bart *et al.*, 1999) do not show a clear correlation between sediment calibre and slope angle (Fig. 16B). They have lower slope angles for the same mixtures of sediment as the linear profiles, probably because they do not rest at the angle-of-repose.

### Controls on slope curvature

The goal of studying the curvature of submarine slopes is to improve the interpretation of the geometry of clinoforms in seismic sections in terms of depositional environment. It has been proposed in an earlier paper that sigmoidally curved slope profiles result from the interference of wave-dominated shelf transport with gravity-driven slope transport at the upper portion of the slope, and that this interference might be the result of base-level fluctuations (Adams & Schlager, 2000).

The morphology of the seven lacustrine deltas in this study supports this hypothesis. They all have sharp breaks between the delta plain and slope, and linear or exponential profiles. Sigmoidal profiles are conspicuously absent. This is expected in such an alpine setting: the relief is high and steep, sediment supply is high and thus the rate of delta progradation is high. On the other hand, fluctuations in base-level are small: the climate is humid, and the lake basins remain filled with minimal fluctuations in lake level; wave base is very shallow and fluctuates little because the lakes are small and protected by mountains.

Fjord deltas have a more or less similar setting to alpine lakes. The difference is that they are influenced by tides. The Alta delta in Norway (Corner *et al.*, 1990) is sheltered and sand dominated, the wave energy is low, and the spring tide range is 2.5 m. A Gilbert delta with a steep planar upper slope and a sharp break has been documented. The slope angle is  $35^\circ$ , and the depth of the break is 3–5 m. Another fjord delta, the Bella Coola delta in Canada (Kostaschuk &

McMann, 1983), has an exponential curvature, a tidal range of 6 m and the depth of its break lies at 15 m.

Examples of profiles from deltas facing the open ocean instead of sheltered basins are the Mississippi delta and the Ganges–Brahmaputra delta. Kenyon & Turcotte (1985) showed that the Mississippi delta has an exponential curvature. The tidal range in the Gulf of Mexico is less than 0.5 m (Bearman, 1989). An example of a storm-dominated delta is the Ganges–Brahmaputra delta (Kuehl *et al.*, 1997). The progradation rate and composition of this delta are similar to that of the Rhine delta; 15 m per year and dominated by sand and silt (Müller, 1966; Michels *et al.*, 1998). However, the Ganges–Brahmaputra delta, which is storm dominated, has a sigmoidal profile. This can be attributed to the strongly fluctuating depth range of wave action.

In the present paper, the hypothesis of whether the sigmoidal profiles can be explained by the interference of wave-dominated shelf transport with gravity-driven slope transport is explored. The results presented here are compatible with this hypothesis; the Swiss lacustrine deltas and the fjord deltas quoted above have low wave energy and thus stable base levels; the resulting shelf breaks are sharp and the upper slopes are exponential or linear in curvature. The Ganges–Brahmaputra delta, on the other hand, is subjected to strong and highly varying wave action. Consequently, the depth zone of interference between wave-dominated shelf transport and gravity-driven slope transport is wide, and the resulting profile is distinctly sigmoidal. Important in this comparison, both the Rhine delta and the Ganges–Brahmaputra delta prograde at similar rates, and supply per unit area is nearly equal. If supply differs significantly, it needs to be considered in this comparison (Adams *et al.*, 1998, p. 140).

## CONCLUSIONS

1. The curvatures of lacustrine deltas of Swiss lakes are linear or exponential, which represent planar or concave morphologies respectively. All observed breaks between the topset delta plain and the slope are sharp.

2. The planar shape of the upper slope is interpreted as resulting from sediment being deposited at the angle-of-repose. The slope inclination is fixed for these systems, being related to sediment texture, and the sediment transport rate

adjusts to maintain these maximum slope inclinations. Sediment transported by avalanches on the upper slope comes to rest at the non-critical exponential lower slope.

3. The exponential curvature of the lower part of the slope is attributed to the exponential decay of transport capacity or competence of the significant transport mechanisms. The deviation from the exponential trend at the distal end of the slope is attributed to the onset of ponded turbidite deposition, raising the basin floor above the predicted trend.

4. The slope angle of planar profiles shows a correlation with sediment calibre. Exponential profiles do not show a clear correlation between sediment calibre and slope angle; they do not rest at the angle-of-repose, and different sediments can rest at the same slope angle.

5. The absence of sigmoidal profiles on the Swiss deltas is attributed to the high rate of progradation coupled with weak wave action and thus small fluctuations in base level.

## ACKNOWLEDGEMENTS

We thank William Anderson for his help with the seismic survey on Lake Uri, and Mike Sturm, Daniel Ariztegui, Oliver Schmidt and Alois Zwysig for their help with the seismic survey on Lake Brienz. The Swiss National Hydrological and Geological Survey and especially Christian Koch are acknowledged for providing us with the lake level data published in this paper. The Internationale Rheinregulierung, Bauleitung Lustenau, provided us with the bathymetric data for Lake Constance. We would like to thank Robert M. Carter and George Postma for their reviews. The Vrije Universiteit Industrial Associates in Sedimentology provided partial support for this study.

## REFERENCES

- Adams, E.W. and Schlager, W. (2000) Basic types of submarine slope curvature. *J. Sed. Res.*, **70**, 814–828.
- Adams, E.W., Schlager, W. and Wattel, E. (1998) Submarine slopes with an exponential curvature. *Sed. Geol.*, **117**, 135–141.
- Allen, J.R.L. (1970) The avalanching of granular solids on dune and similar slopes. *J. Geol.*, **78**, 326–351.
- Bak, P., Tang, C. and Wiesenfeld, K. (1988) Self-organized criticality. *Phys. Rev. A*, **38**, 364–374.
- Bart, P.J., De Batist, M. and Jokat, W. (1999) Interglacial collapse of Cray Trough-Mouth Fan, Weddell Sea, Antarctica:

- implications for Antarctic glacial history. *J. Sed. Res.*, **69**, 1276–1289.
- Bearman, G.** (1989) *Waves, Tides, and Shallow Water Processes*. The Open University and Butterworth-Heinemann, Walton Hall, Milton Keynes, 187 pp.
- Bogen, J.** (1983) Morphology and sedimentology of deltas in fjord and fjord valley lakes. *Sed. Geol.*, **36**, 245–267.
- Carter, R.M.** (1988) Post-breakup stratigraphy of the Kaikoura Synthem (Cretaceous–Cenozoic), continental margin, southeastern New Zealand. *NZ J. Geol. Geophys.*, **31**, 405–429.
- Chandler, R.J.** (1973) The inclination of talus, arctic talus terraces, and other slopes composed of granular materials. *J. Geol.*, **81**, 1–14.
- Corner, G.D., Nordhal, E., Munch-Ellingsen, K. and Robertsen, K.R.** (1990) Morphology and sedimentology of an emergent fjord-head Gilbert-type delta: Alta delta Norway. In: *Coarse-Grained Deltas* (Eds A. Colella and D.B. Prior), *Int. Assoc. Sedimentol. Spec. Publ.*, **10**, 155–168.
- De Batist, M., Bart, P.J. and Miller, H.** (1997) Trough-mouth fans: Cray Fan, eastern Weddell Sea, Antarctica. In: *Glaciated Continental Margins: an Atlas of Acoustic Images* (Eds T.A. Davies, T. Bell, A.K. Cooper, H. Josenhans, L. Polyak, A. Solheim, M.S. Stoker and J.A. Stravers), pp. 276–279. Chapman & Hall, London.
- Driscoll, N.W. and Karner, G.D.** (1999) Three-dimensional quantitative modeling of clinoform development. *Mar. Geol.*, **154**, 383–398.
- Finckh, P. and Kelts, K.** (1976) Geophysical investigations into the nature of pre-Holocene sediments of Lake Zurich. *Eclogae Geol. Helv.*, **69**, 139–148.
- Finckh, P., Kelts, K. and Lambert, A.** (1984) Seismic stratigraphy and bedrock forms in perialpine lakes. *Geol. Soc. Am. Bull.*, **95**, 1118–1128.
- Förstner, U., Müller, G. and Reineck, H.-E.** (1968) Sedimente und Sedimentgefüge des Rheindeltas im Bodensee. *Neues Jb. Mineral. Abh.*, **109**, 33–62.
- Gilbert, G.K.** (1890) *Lake Bonneville*. US Geol. Surv. Monogr., **1**, 438 pp.
- Heezen, B.C., Tharp, M. and Ewing, M.** (1959) *The Floors of the Oceans. I. The North Atlantic*. Geol. Soc. Am. Spec. Pap., **65**, 122 pp.
- Hiscott, R.N.** (1994) Loss of capacity, not competence, as the fundamental process governing deposition from turbidity currents. *J. Sed. Res.*, **A64**, 209–214.
- Hsü, K.J. and Kelts, K.** (1985) Swiss lakes as a geological laboratory, Part I: Turbidity currents. *Naturwissenschaften*, **72**, 315–321.
- Jansa, L.F.** (1991) Lithostratigraphy 10, carbonate buildup morphology. In: *East Coast Basin Atlas Series: Scotian Shelf* (Ed. J.L. Bates), Atlantic Geoscience Centre, Geological Survey of Canada, **69**.
- Kenter, J.A.M.** (1990) Carbonate platform flanks: slope angle and sediment fabric. *Sedimentology*, **72**, 777–794.
- Kenyon, P.M. and Turcotte, D.L.** (1985) Morphology of a delta prograding by bulk sediment transport. *Geol. Soc. Am. Bull.*, **96**, 1457–1465.
- Kirkby, M.J.** (1987) General models of long-term slope evolution through mass movement. In: *Slope Stability, Geotechnical Engineering and Geomorphology* (Eds M.G. Anderson and K.S. Richards), pp. 359–379. John Wiley and Sons, London.
- Kostaschuk, R.A. and McMann, S.B.** (1983) Observations on delta-forming processes in a fjord-head delta, British Columbia, Canada. *Sed. Geol.*, **36**, 269–288.
- Kuehl, S.A., Levy, B.M., Moore, W.S. and Allison, M.A.** (1997) Subaqueous delta of the Ganges-Brahmaputra river system. *Mar. Geol.*, **144**, 81–96.
- Matter, A., Süssstrunk, A.E., Hinz, K. and Sturm, M.** (1971) Ergebnisse reflexionsseismischer Untersuchungen im Thunersee. *Eclogae Geol. Helv.*, **64**, 505–520.
- Matter, A., Desolin, D., Sturm, M. and Süssstrunk, A.E.** (1973) Reflexionsseismische Untersuchung des Brienzersees. *Eclogae Geol. Helv.*, **66**, 71–82.
- Meixner, H.** (1991) *Das Rheindelta im Bodensee: Seegrundaufnahme vom Jahre 1989*. Internationale Rheinregulierung, Bauleitung Lustenau, 18 pp.
- Michels, K.H., Kudrass, H.R., Hübscher, C., Suckow, A. and Wiedlicke, M.** (1998) The submarine delta of the Ganges-Brahmaputra: cyclone-dominated sedimentation patterns. *Mar. Geol.*, **149**, 133–154.
- Mosher, D.C., Moran, K. and Hiscott, R.N.** (1994) Late Quaternary sediment, sediment mass flow processes and slope stability on the Scotian Slope, Canada. *Sedimentology*, **41**, 1039–1061.
- Müller, G.** (1966) The New Rhine Delta in Lake Constance. In: *Deltas in Their Geologic Framework* (Eds M.L. Shirley and J.E. Ragsdale), pp. 107–124. Houston Geological Society, Houston, TX.
- Müller, G. and Gees, R.A.** (1970) Distribution and thickness of Quaternary sediments in the Lake Constance Basin. *Sed. Geol.*, **4**, 81–87.
- Nemec, W.** (1990a) Aspects of sediment movement on steep delta slopes. In: *Coarse-Grained Deltas* (Eds A. Colella and D.B. Prior), *Int. Assoc. Sedimentol. Spec. Publ.*, **10**, 29–73.
- Nemec, W.** (1990b) Deltas – remarks on terminology and classification. In: *Coarse-Grained Deltas* (Eds A. Colella and D.B. Prior), *Int. Assoc. Sedimentol. Spec. Publ.*, **10**, 3–12.
- Orton, G.J. and Reading, H.G.** (1993) Variability of deltaic processes in terms of sediment supply, with particular emphasis on grain size. *Sedimentology*, **40**, 475–512.
- Pirmez, C., Pratson, L.F. and Steckler, M.S.** (1998) Clinoform development by advection–diffusion of suspended sediment: modeling and comparison to natural systems. *J. Geophys. Res.*, **103**, 24 141–24 157.
- Postma, G.** (1990) Depositional architecture and facies of river and fan deltas: a synthesis. In: *Coarse-Grained Deltas* (Eds A. Colella and D.B. Prior), *Int. Assoc. Sedimentol. Spec. Publ.*, **10**, 13–27.
- Prior, D.B. and Bornhold, B.D.** (1990) The underwater development of Holocene fan deltas. In: *Coarse-Grained Deltas* (Eds A. Colella and D.B. Prior), *Int. Assoc. Sedimentol. Spec. Publ.*, **10**, 75–90.
- Ross, W.C., Watts, D.E. and May, J.A.** (1995) Insights from stratigraphic modeling: mud-limited versus sand-limited depositional systems. *AAPG Bull.*, **79**, 231–258.
- Schlager, W. and Camber, O.** (1986) Submarine slope angles, drowning unconformities, and self erosion of limestone escarpments. *Geology*, **14**, 762–765.
- Schlager, W. and Chermak, A.** (1979) Sediment facies of platform-basin transition, Tongue of the Ocean, Bahamas. In: *Geology of Continental Slopes* (Eds L.J. Doyle and O.H. Pilkey), *SEPM Spec. Publ.*, **27**, 193–208.
- Schmidt, O.I.** (1998) *Brienzersee Turbiditäreignis vom Frühjahr 1996*. Diplomthesis, ETH Zürich, Switzerland.
- Siegenthaler, C. and Sturm, M.** (1991) Slump induced surges and sediment transport in Lake Uri, Switzerland. *Verh. Int. Ver. Theor. Angew. Limnol.*, **24**, 955–958.

- Sly, P.G.** (1978) Sedimentary processes in lakes. In: *Lakes: Chemistry, Geology, Physics* (Ed. A. Lerman), pp. 65–89. Springer-Verlag, New York.
- Sturm, M.** (1976) Die Oberflächensedimente des Brienzersees. *Eclogae Geol. Helv.*, **69**, 111–123.
- Sturm, M.** and **Matter, A.** (1972) Sedimente und Sedimentationsvorgänge im Thunersee. *Eclogae Geol. Helv.*, **65**, 563–590.
- Sturm, M.** and **Matter, A.** (1978) Turbidites and varves in Lake Brienz (Switzerland): deposition of clastic detritus by density currents. In: *Modern and Ancient Lake Sediments*

(Eds A. Matter and M.E. Tucker), *Int. Assoc. Sedimentol. Spec. Publ.*, **2**, 147–168.

- Vanney, J.R.** and **Stanley, D.J.** (1983) Shelfbreak physiography: an overview. In: *The Shelfbreak: Critical Interface on Continental Margins* (Eds D.J. Stanley and G.T. Moore), *SEPM Spec. Publ.*, **33**, 1–24.

*Manuscript received 26 April 2000;*  
*revision accepted 5 January 2001.*